



**HAL**  
open science

## Spurious molecular beams in Knudsen effusion mass spectrometry

Christian Chatillon, Ioana Nuta

► **To cite this version:**

Christian Chatillon, Ioana Nuta. Spurious molecular beams in Knudsen effusion mass spectrometry. *Calphad*, 2019, 65, pp.8-15. <10.1016/j.calphad.2019.01.009>. <hal-02405380>

**HAL Id: hal-02405380**

**<https://hal.science/hal-02405380v1>**

Submitted on 21 Oct 2021

**HAL** is a multi-disciplinary open access archive for the deposit and dissemination of scientific research documents, whether they are published or not. The documents may come from teaching and research institutions in France or abroad, or from public or private research centers.

L'archive ouverte pluridisciplinaire **HAL**, est destinée au dépôt et à la diffusion de documents scientifiques de niveau recherche, publiés ou non, émanant des établissements d'enseignement et de recherche français ou étrangers, des laboratoires publics ou privés.



Distributed under a Creative Commons CC BY-NC 4.0 - Attribution - Non-commercial use - International License

## Spurious molecular beams in Knudsen Effusion Mass Spectrometry

Christian CHATILLON and Ioana NUTA

*University Grenoble Alpes, CNRS, Grenoble INP, SIMAP*

*38000 Grenoble - France*

### 1 Introduction

The Knudsen effusion method is now a relatively old method born at the beginning of the twentieth century (1904) as summarized by Cater [1] at the NBS – Gaithersburg meeting in 1977. The coupling with a mass spectrometer was performed in 1954 by different research teams as compiled and presented by Inghram et Drowart [2] at the Asilomar meeting (1964) in order to analyze the composition of the vapors in equilibrium with a heated sample. Some smart efforts were done in the seventies and eighties in order to elucidate the real nature of the collected effusion beams by any detectors including the mass spectrometers in relation with different physico-chemical phenomena occurring at the effusion orifice or near the edges of these orifices such as spurious molecular flows as summarized by Drowart et al [3] in a special technical report of IUPAC dedicated to the so-called Knudsen Cell Mass Spectrometric method (KCMS). The present work summarizes the origin of these spurious molecular flows in relation with research works that detected and studied these flows, analyzes the capability of the so-called “restricted collimation device” to discard them in the course of vapor pressure and activity determinations by the KCMS method and finally proposes new analytical techniques to detect and quantify these flows in the course of mass spectrometric experiments.

#### Theory/calculations

##### 1.1 Conventional coupling with mass spectrometry

The effusion flow of any gaseous species at low pressure through an orifice under vacuum is a well-known process since the original works by Knudsen in 1909[4]. For an orifice with a very thin edge, the emission of a molecule in a  $\theta$  direction from the normal to the orifice (Figure 1) included in a volume adjacent to the orifice and defined by the orifice area  $ds$  and the mean velocity  $\bar{v}$  of the molecules and towards a direction  $\theta$  in an elementary solid angle  $d\Omega$  is written according to the following relation,

$$\frac{dN}{dt}(\theta) = n\bar{v} ds \cos \theta \frac{d\Omega}{4\pi} \quad (1)$$

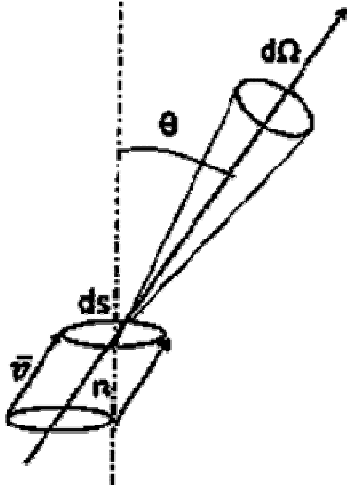


Figure 1 Emission of a molecule under vacuum through a thin edge orifice of  $ds$  area in a direction  $\vartheta$  and under an elementary solid angle  $d\Omega$ .

in which the ratio  $d\Omega/4\pi$  is the probability of emission in the elementary solid angle reported to the full space since the molecules in the gas phase travel in any direction. This relation results from the gas kinetic theory. Integration in the full space outside the Knudsen cell leads to the well-known Hertz-Knudsen relation,

$$\frac{dN}{dt} = \frac{p s}{\sqrt{2\pi MRT}} \quad (2)$$

$p$  being the pressure in the cell under the orifice,  $s$  the orifice section,  $M$  the molar mass of the effused molecule,  $R$  the gas constant and  $T$  the temperature of the cell. When coupling an effusion cell to a mass spectrometer ion source, the integration is performed between the effusion orifice and the entrance aperture of the ionization chamber as shown in Figure 2.

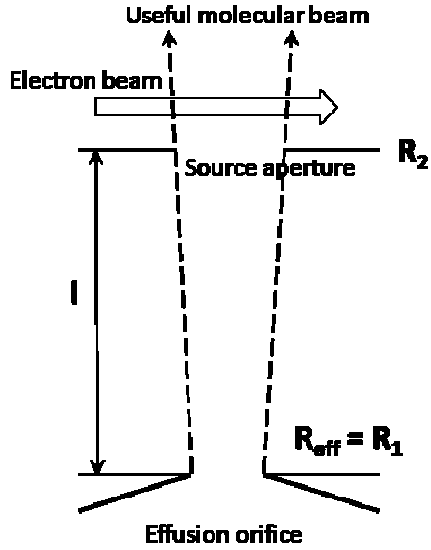


Figure 2 Coupling of an effusion orifice with the aperture of the ionization chamber of a mass spectrometer. Useful and genuine molecular beam exchanged between the effusion orifice and the ion source aperture.  $R_{eff}$ ,  $R_1$  and  $R_2$  are apertures radii.

The elementary solid angle between two elementary surfaces  $ds_1$  and  $ds_2$  on each aperture – effusion orifice and source aperture - is,

$$d\Omega = \frac{ds_1 \cos\theta_1 ds_2 \cos\theta_2}{l^2} \quad (3)$$

and the number of molecules exchanged between the effusion orifice and the source aperture is obtained by integration,

$$\frac{dN}{dt} = \frac{p}{\sqrt{2\pi MRT}} \cdot \frac{1}{\pi} \cdot \iint_0^{R_1 R_2} \frac{ds_1 \cos\theta_1 ds_2 \cos\theta_2}{l^2} \quad (4)$$

and according to Vassent et al [5] this relation becomes,

$$N(t) = \frac{p}{\sqrt{2\pi MRT}} \cdot \frac{\pi}{2} \cdot \left[ (l^2 + R_1^2 + R_2^2) - \sqrt{(l^2 + R_1^2 + R_2^2)^2 - 4R_1^2 R_2^2} \right]. \quad (5)$$

This relation gives the flow of genuine molecules (moles /s) than will pass through the ionization chamber and coming from the only vapor phase in equilibrium under the effusion orifice *i.e.* with a pressure  $p$ . The optimization of the genuine effusion flow is directly related to the distance  $l$  as shown in Figure 3. In a conventional Knudsen cell mass spectrometer the distance  $l$  is built as short as possible taking into account on the high voltage of the ion source (5000 to 10000 V) and on the necessity of a cooling plate interposed between the effusion furnace and the ion source.

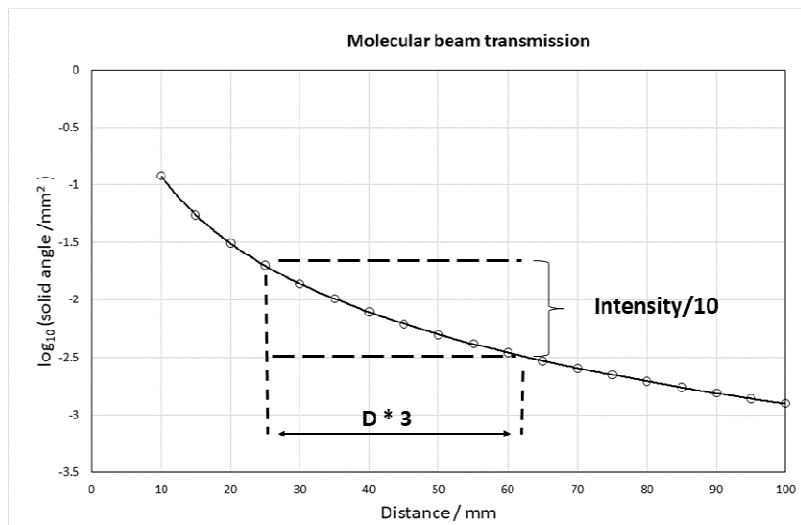


Figure 3 Influence of the effusion orifice – ionization chamber aperture distance on the molecular beam yield at the level of the ionization. Increasing the distance by a factor 3 decreases the molecular beam intensity by a factor 10.

In early times when using twin or multiple cells for the direct determination of pressures ratio i.e. ionic intensities ratio between two or more effusion cells leading to activity measurements[6], the basic test of the method relied on the measurements with the same material in each cells. So doing measured ratios would have to be the same for same orifices, or slightly different for different orifices as for instance published by Chatillon et al [7] with Ag in each cells as presented in Figure 4. Four identical cells were located in a “real” isothermal envelop specially built with heat pipes (Chatillon et al [7]) and differences up to  $\pm 1$  to 2% were observed however the four effusion holes were measured with an accuracy better than 0.2%. More, these differences were not significantly reduced at the melting temperature plateau of silver – a temperature plateau as observed during a long time by mass spectrometry which is strictly equal for each cell -. The conclusion was that the difference in cells temperature was not the cause for differences in ionic intensities as measured. We therefore have to explore other causes that may produce a spurious molecular beam added to the genuine molecular beam associated to the equilibrium in effusion cells.

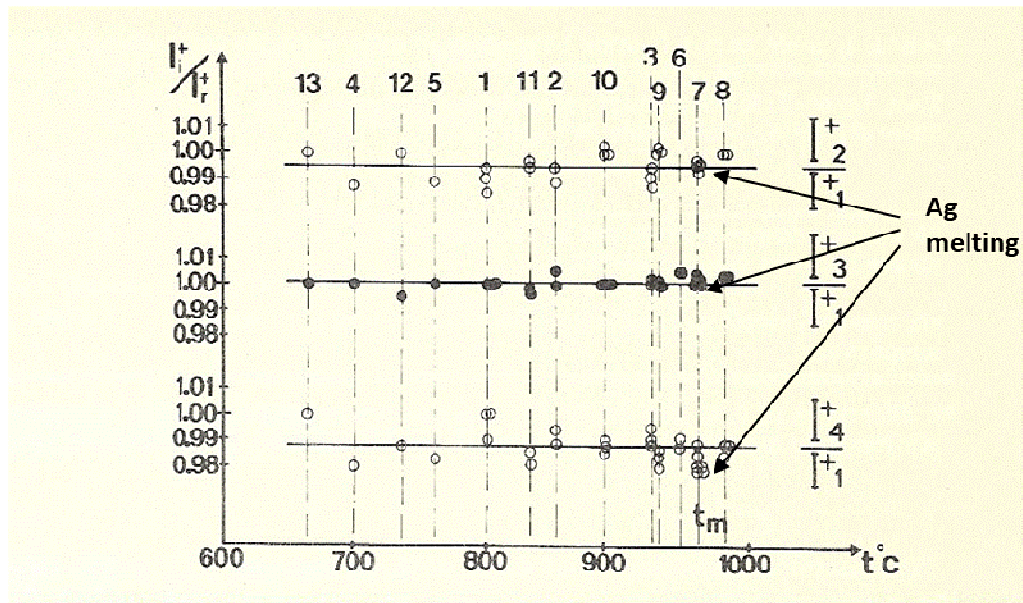


Figure 4 Ratio of ionic intensities- referred to cell 1 - measured with four identical effusion cells – crucible + lid - loaded with the same Ag sample and located in an isothermal heat-pipe envelop. Numbers at the top are the sequences of measurements as a function of temperature when starting from the beginning of the experiment (1) to the end (13).

The environment of the effusion cell coupled with the mass spectrometer is presented in Figure 5, when going from the principle to the realization.

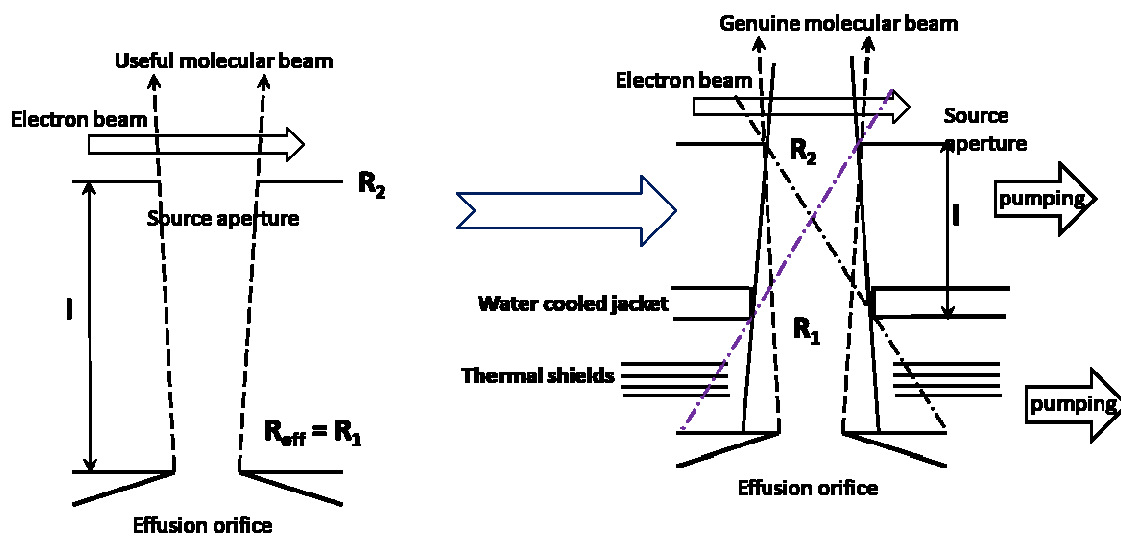


Figure 5 From the principle of mass spectrometric detection of a genuine effusion beam to the real device combining genuine and spurious beams.  $R_{eff}$ ,  $R_1$  and  $R_2$  are apertures radii.

The effusion cells are generally located in a furnace with a set of thermal shields and a separation into two housings – one for the ion source, the other for the furnace – fitted with two different UHV pumping

systems. The background pressure in the furnace housing due to degassing and sometimes also to the nature of the effused beam – when permanent gases are effused - is generally higher than the one in the ion source housing. More, the background pressure in the source housing must be as low as possible to reduce the masses interferences in the spectrum that correspond to unresolved species. So the aperture between the two compartments must be small and the pumping capacities well adapted.

As shown in Figure 5 when drawing the umbra and penumbra zones for molecules going in straight line (without collisions), the aperture on the cold trap (water jacket) let the ionization chamber detect molecular beams coming from the edges of the effusion orifice as well as from thermal shields. Different phenomena can provide flow of molecules arriving in these zones that can be re-emitted.

- The effusion cell provides molecules along the normal to the effusion orifice that travel to the ion source with a very small solid angle – generally  $<10^{-2}$  steradian – and the main part of the molecular beam -  $> 98\%$  and about  $2\pi$  steradian - goes in the thermal shields and in the furnace. The set of thermal shields (the casing) (Figure 6 ) acts as a surrounding effusion cell that condenses and evaporates parts of the initial molecular beam. A steady-state equilibrium is built in the casing that results in a steady-state pressure of the initially effusing molecules according to the so-called “thermo-molecular effect”[8], meanwhile part of the molecules condensates due to the lower temperature of the first thermal shield than of the effusion orifice. The thermos-molecular relation between these flows is,

$$\frac{P_i \cdot S_{\text{eff}}}{\sqrt{2\pi M_i R T_{\text{cell}}}} = F_{\text{Cond}}^{T_{\text{shield}}} + \frac{P_i \cdot S_{\text{shield}}}{\sqrt{2\pi M_i R T_{\text{shield}}}} \quad (6)$$

when no transformation (decomposition) of the molecules occurs. The surfaces  $s$  are the apertures. In order to obtain isothermal conditions for the effusion cell, the number of thermal shields is important (10 in our devices), and their apertures minimized. Consequently, the mean temperature in the first shield of the casing around the effusion cell is not very different from the cell, i.e. within 100 to 200°C lower than the effusion cell temperature. Chatillon et al[9] evaluated the surface re-vaporization to about 2 – 5% around the effusion orifice reported to the value 1 for the emission at the effusion orifice. Note that this value can be strongly modified when decomposition of molecules as well as reactions with furnace materials occurs especially when high volatile species exist in the molecular beam with the higher partial pressure (ex:  $P_2$ , or  $P_4$ , molecules effusing from InP - in the following study in reference[10] - that condense as pure phosphorus extremely volatile on the thermal shields).

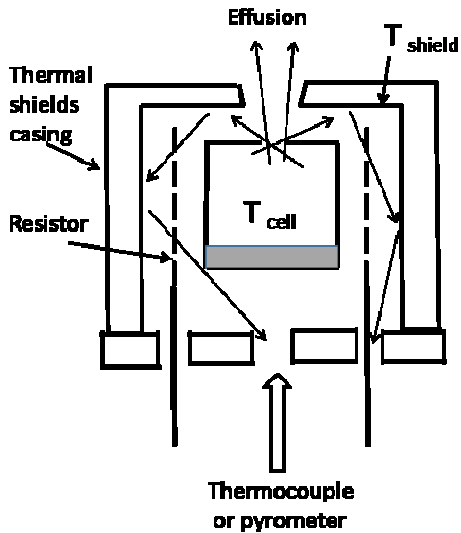


Figure 6 Schematics of the different molecular flows following the effusion flow and existing at a steady-state pressure in the thermal shields casing.

- Surface diffusion of adsorbed molecules at saturation on the cell walls occurs along the orifice walls and from its external edge[9] that provides molecular emission of the orifice sides towards the source aperture as presented in Figure 7. Due to the very large difference in chemical potential between the vapor saturated inside the cell and the unsaturated vapor in outside vacuum, the surface diffusion along the orifice walls is always occurring as studied by Winterbottom et al [11, 12] – this phenomenon is a steady-state process occurring with the effusion process -. Indeed, after the study of this phenomenon using Monte-Carlo calculations, Ward et al [13-17] proposed to decrease this flow relative to total effusion flow by enlarging the effusion area and using cylindrical orifices to already decrease the adsorbed concentration at edges contrarily to the general rule of thin edge orifices devices used in earlier studies following Knudsen original works. The decrease of the surface emissivity from the orifice edge depends also on the lid material *via* its physico-chemical interaction with the vapors (diffusion coefficient and Gibbs energy of desorption).

In order to evaluate the contribution of surface diffusion to the total matter flow lost by an effusion cell, some works were undertaken using different cells materials for the effusion orifices. Normally, 2<sup>nd</sup> and 3<sup>rd</sup> laws calculations would produce different enthalpy results and the 2<sup>nd</sup> law being more sensitive to surface diffusion contributions would produce smaller enthalpy values as predicted by Winterbottom et al [11,12]. However, their 2<sup>nd</sup> and 3<sup>rd</sup> law interpretations were not able to show what was the “best” choice for the material. Note that the surface diffusion flow associated to atomic or molecular adsorption on orifice walls is different from bulk “creeping” (sometimes called “overflow”) coming from liquid or glassy samples in the sense that this phenomenon may be a batch process – occurring above some temperature threshold – or random during the experiment as stated by Cater[1].

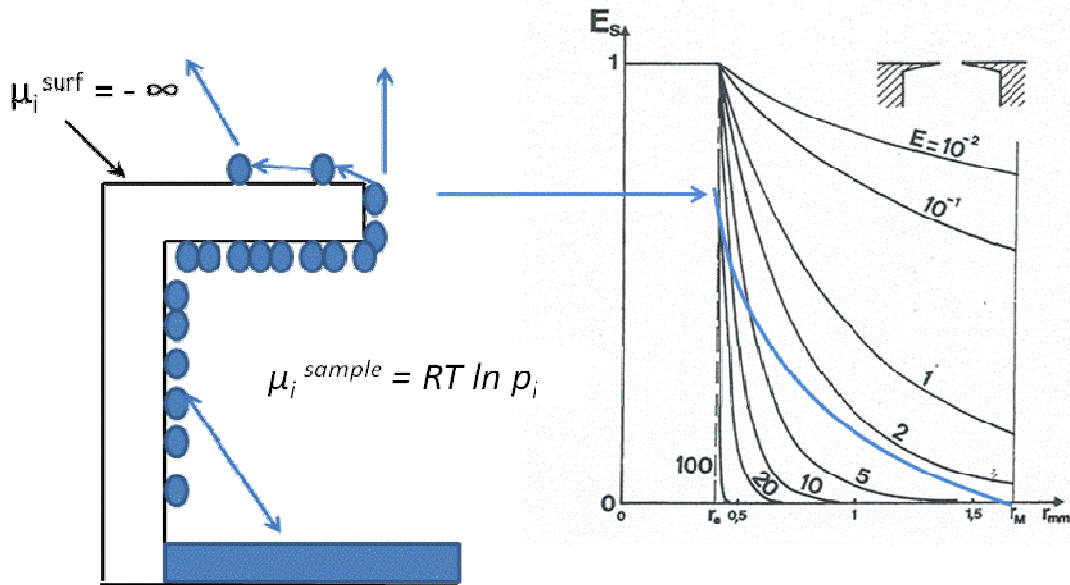


Figure 7 Surface diffusion along the orifice walls provide adsorbed molecules to feed the edge of the orifice and surface emission of the edge sides by desorption of molecules (or atoms) towards the source aperture.

Since the beginning of the Knudsen cell mass spectrometer coupling, researchers [2, 18, 19] were conscious of the importance of these phenomena and analytic devices consisting of slits or blades interposed on the trajectory of the molecules between the cell orifice and the source aperture were used to monitor the appearance or the importance of these parasitic flows as shown in Figure 8.

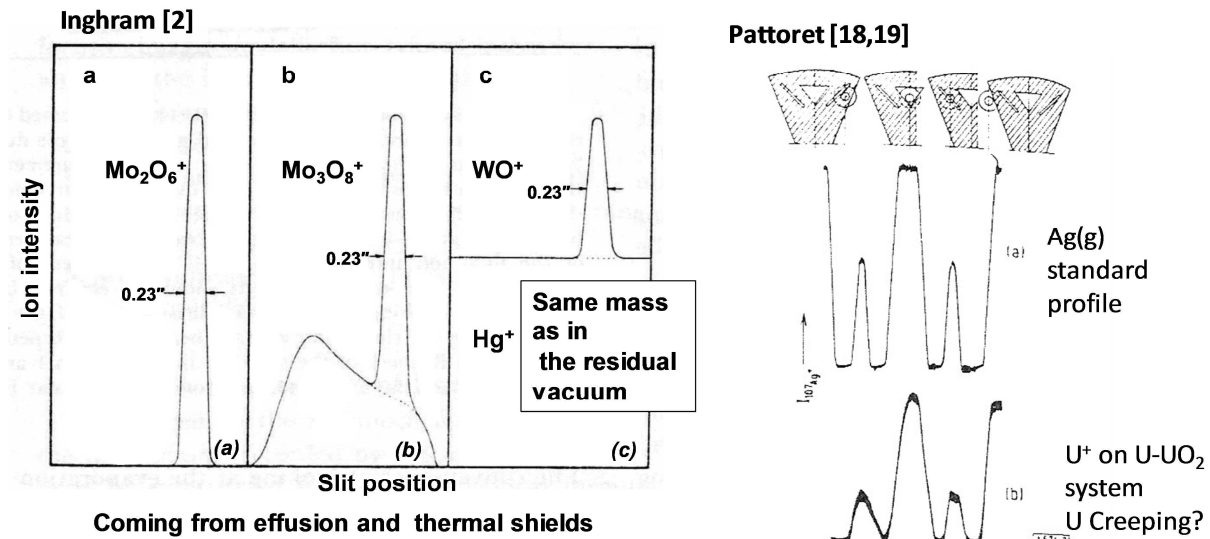


Figure 8 Surface vaporization around the effusion orifice edge as analyzed with a slit scanning the molecular beam perpendicularly to its normal to the orifice on the trajectory of molecules.

Same analysis was also performed systematically with blades by Chatillon et al [9] in order to evaluate quantitatively the surface contribution relative to the genuine effusion contribution as detected by the mass spectrometer. In reality a quantitative approach is possible for the only surface emissivity that is practically constant as for instance for molecules providing from the multiple reflections on thermal

shields. For surface emissivity due to surface diffusion, the emissivity profile is too sharp to be analyzed with a blade or a slit meanwhile the contribution to the total flow remain non negligible.

For this reason, and in view of performing activity measurements, Martin-Garin et al[20] decided to implement a restricted collimation device that discard definitely all these surface contributions in the mass spectrometric detection.

## 1.2 Restricted collimation device in mass spectrometry

The restricted collimation concerns the collimation of the Knudsen molecular beam issued from the effusion orifice in such a manner that the only vapors introduced into the ionization chamber – *i.e.* passing through its molecular beam entrance aperture – are coming from the inner vapor phase of the Knudsen cell. The principle of the device is presented in Figure 9 showing the role of the two

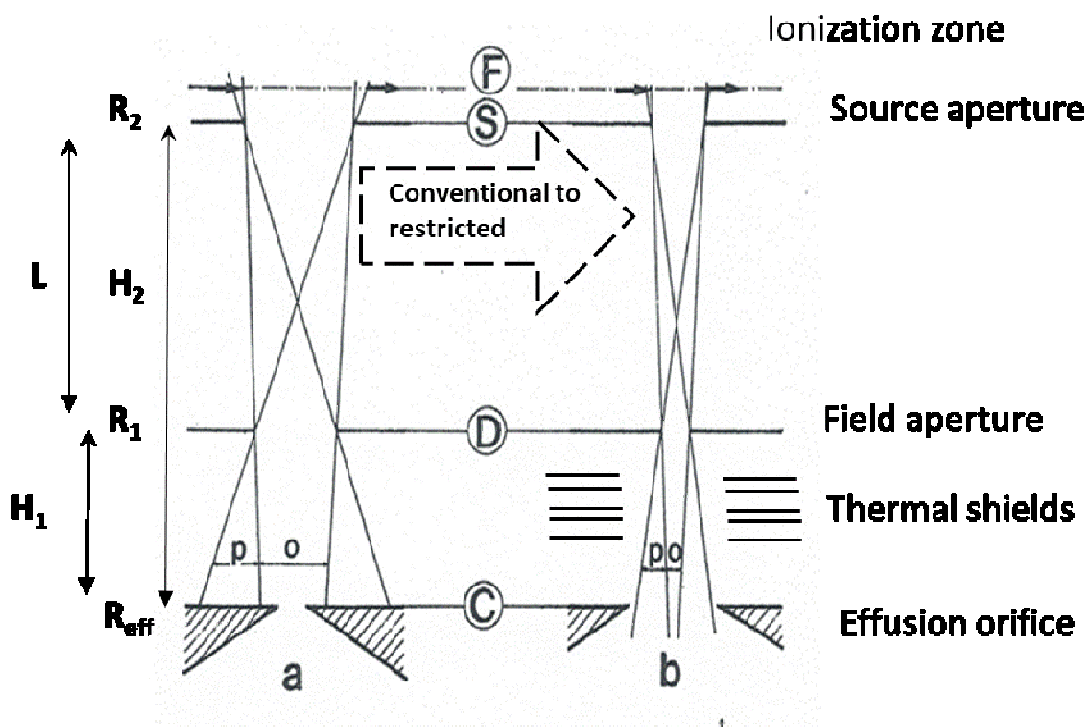


Figure 9. Disposition of the two apertures – field and source – from a conventional molecular beam sampling device to a restricted one. The Umbra (o) and penumbra (p) zones as defined for species travelling in straight lines without collisions show the location of the emitted molecules towards the ionization chamber.

apertures: - (i) the first one located just above the effusion orifice or Knudsen furnace, - (ii) the second at the entrance of the ionization chamber. The prerequisites for building such a restricted collimation have been published by Morland et al [18] and especially the optimization of the molecular transmission from the effusion orifice to the ionization chamber. The molecular flow (molecular transmission) is calculated starting from the solid angle sustained by the two apertures field and source:

$$F_i = \frac{p_i}{\sqrt{2\pi M_i RT}} \cdot \frac{\pi}{2} \cdot \left( (L^2 + R_1^2 + R_2^2) - \sqrt{(L^2 + R_1^2 + R_2^2)^2 - 4R_1^2 R_2^2} \right). \quad (7)$$

In this relation  $p_i$  is the partial pressure of the species  $i$  in the cell, the first factor is the Knudsen relation for an orifice (thin walls) of one unit of surface, and the second and third factors are the solid angle that characterizes the geometrical probability for passing through the collimation device from the cell to the source: this factors can be called “transmission factor”. In the mass spectrometer a certain geometrical configuration is fixed when building the apparatus, and the choice of the collimation device has to be optimized. When performing an experiment, the following factors are fixed:

- The effusion orifice radius  $R_{\text{eff}}$  (and Clausing coefficient) is fixed to a minimum value that favors equilibrium conditions in the cell for vaporization. Usually the pertinent ratio  $f = sC/S - S$  being either the evaporation surface of the sample or the cell section - is the one defined by Motzfeldt[21] when studying non-equilibrium conditions defined by an evaporation (or condensation) coefficient
- $H_1$  (see fig. 9) the distance between the effusion orifice and the field aperture. In case of cylindrical orifices of  $L_{\text{eff}}$  length, this distance becomes  $H_1 + L_{\text{eff}}$
- $H_2$  (see fig. 9) the distance between the effusion orifice and the source aperture. In case of cylindrical orifices of  $L_{\text{eff}}$  length, this distance becomes  $H_2 + L_{\text{eff}}$
- $L = H_2 - H_1$  is fixed when building the mass spectrometer structure
- $D_p$  is the admitted penumbra zone diameter at the level of the effusion orifice molecular entrance for the molecules effusing (for cylindrical orifice take into account of  $L_{\text{eff}}$ ) that is defined as  $D_{\text{eff}} - \text{Clearance}$ . The clearance is the one coming from the mechanical positioning of the effusion cells in front of the collimation axis.

The main remaining parameters are the two apertures diameters that can be varied in view of optimizing the transmission of the molecular beam. When choosing first a source aperture diameter  $D_2$  the corresponding field aperture  $D_1$  (using Thales theorem) becomes for a fixed penumbra diameter  $D_p$ ,

$$D_1 = \left[ D_p \frac{(H_2 - H_1)}{H_2} \right] - \left[ D_2 \frac{H_1}{H_2} \right]. \quad (8)$$

This relation imposes a detection of gaseous species coming from only the inner gas phase in equilibrium with the vaporizing sample. The transmission factor is then calculated and its value (solid angle) calculated and presented as a function of the source aperture diameter in Figure 10.

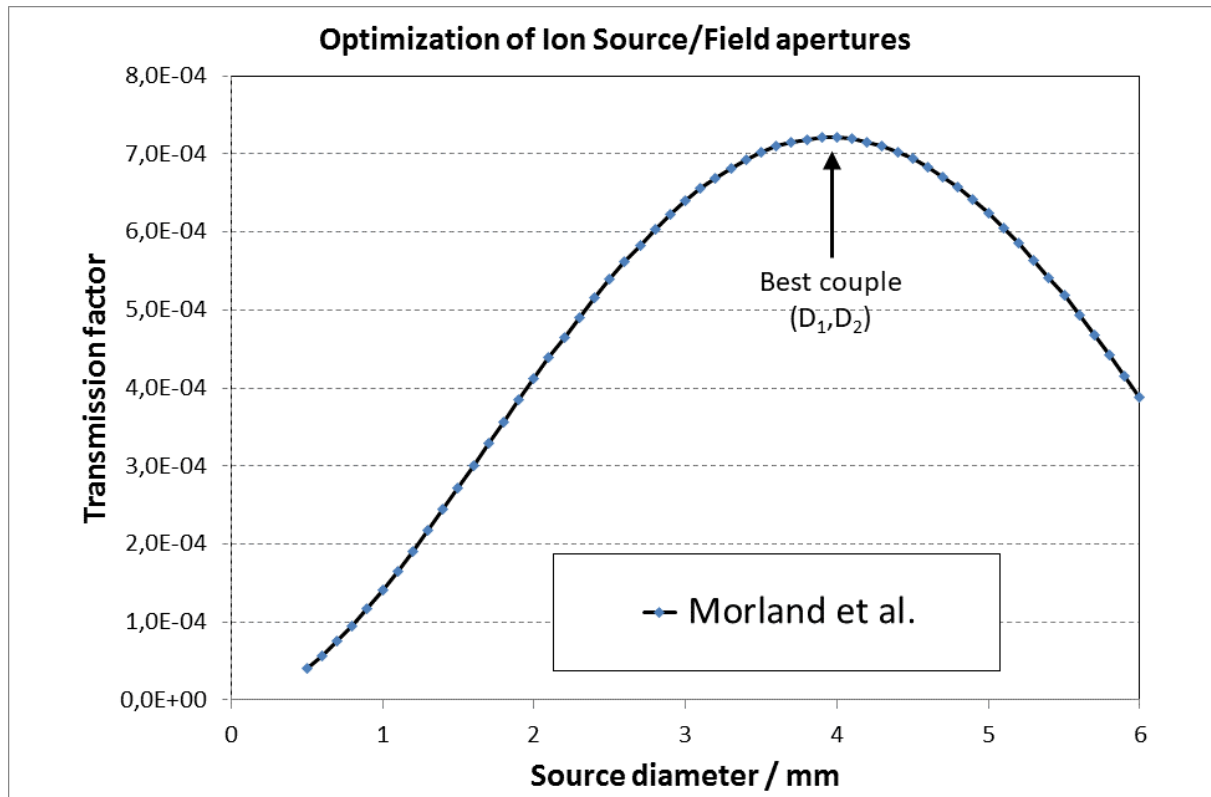


Figure 10 Transmission factor (solid angle for the detected molecular beam) as a function of the source aperture diameter and its correlated (relation (8)) field diameter.

Note that for each source aperture diameter there exist a defined field diameter as discussed and presented by Morland et al [22]. The transmission factor has a maximum that is chosen in building the collimation device: indeed, any mass spectrometer apparatus using restricted collimation device must possess a set of ion source apertures and field apertures that allows matching this maximum.

The influence of the other fixed parameters has been studied by Morland et al [22] for their influence on the transmission factor and in view of determining the best conditions for the building of a mass spectrometer coupled to Knudsen effusion. For a fixed distance  $H_1$  for instance, it was observed as presented in Figure 11 that when the distance  $L=H_2-H_1$  increases, the transmission factor also increases in contrary to what happens in conventional effusion (see Figure 3).

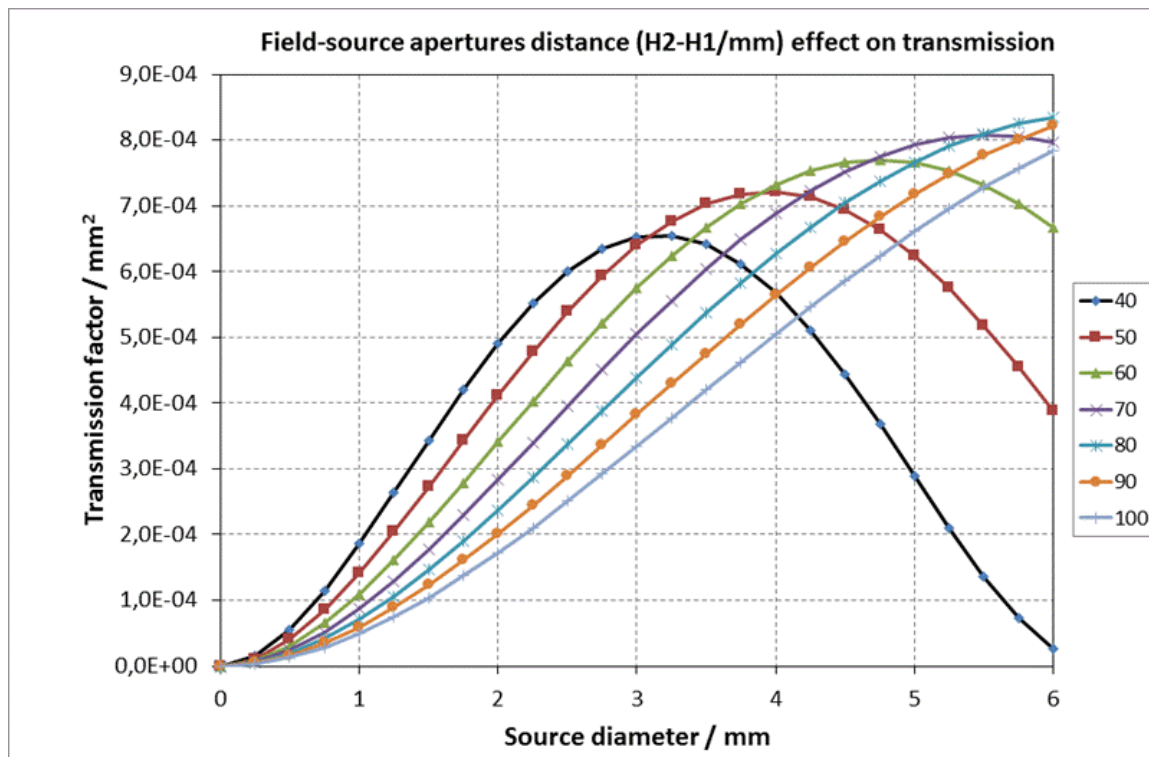


Figure 11 Influence of the distance  $L=H_2-H_1$  as mentioned at the right side in mm on the molecular transmission factor and for a fixed distance  $H_1$  between the effusion orifice and the field aperture. Refer to Figure 9 for the definition of the  $H_1$ ,  $H_2$  terms.

In the work of Morland et al [22], the implicit assumption is that the solid angle as defined by the two field/source apertures (Figure 12) defines any flow of molecules coming from the effusion cell, whatever are located the emitted molecules – effusion orifice (higher pressures for the method  $\sim 10^{-4}$  bar) or from the sample surface (pressures  $< 10^{-7}$  bar) or gas phase for intermediate pressures when collisions occur in the gas phase of the cell where the pressure is assumed to be constant - contrarily to collisions occurring in the molecular beam expansion before detection that are related to the different speeds of the effused species. These last collisions must be treated in a separate calculation.

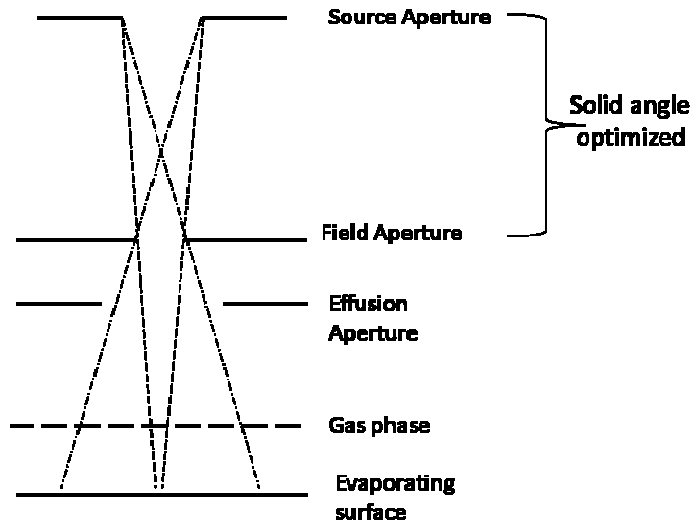


Figure 12 *Optimized solid angle compared to the real level for emission of the gaseous species*

In order to check if the emitted level for the gaseous species has some influence on the transmission factor, recently Nuta and Chatillon [23, 24] calculated by integration from elementary surfaces chosen at any level the flow of gaseous species emitted (in equilibrium conditions) that reach the source aperture and passing through the field aperture. The principle of the integration is presented in Figure 13 and based on the elementary relation,

$$\frac{dN}{dt} = \frac{p}{\sqrt{2\pi MRT}} \cdot \frac{1}{\pi} \frac{ds \cos\theta ds_2 \cos\theta_2}{l^2} \quad (9)$$

that is integrated over the two surface  $S$  and  $S_2$ , with a test at the level of  $S_1$ .

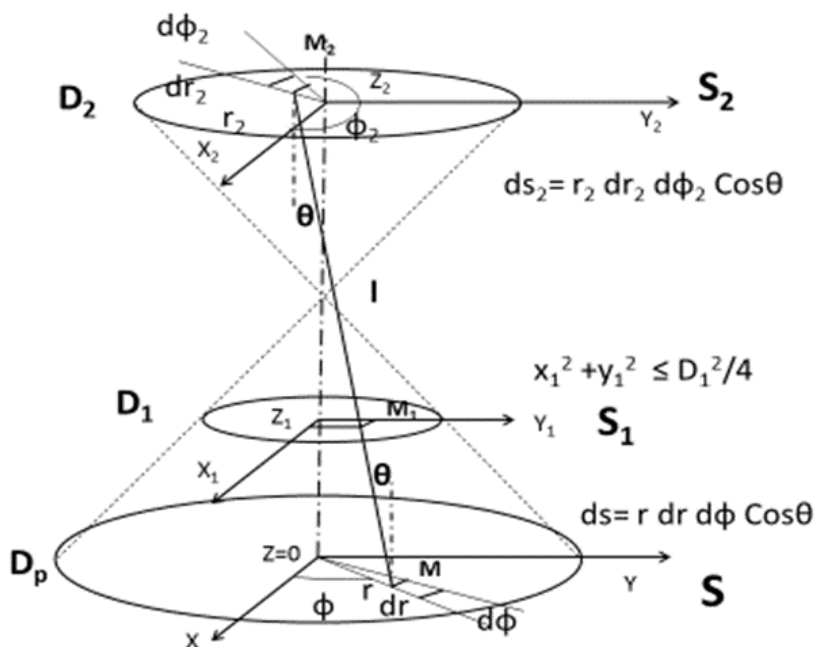


Figure 13 Principle for calculations based on elementary surfaces for the molecular transmission factor (solid angle). A test is performed for species passing through the field aperture  $D_1$ .

The first calculations by Nuta and Chatillon[23] indicated that the transmission varied with the distance between  $S$  and  $S_1$ , but at that time Radke et al [25, 26] by Monte Carlo calculations found that the transmission was constant. Nuta and Chatillon [24] checked the early calculations and found a transcription error in the software, and checked effectively that the distance no more influence the transmission – and this feature confirmed that the Morland et al [22] assumption of a constant solid angle (transmission) for the restricted collimation is valuable whatever the emission of gaseous species is located.

The present integration supposes that the gaseous species do not have some collisions in their trajectory between the emission and their entrance in the ionization chamber coming either from other species in the gas phase of the cell, or with other species along their trajectory from emission to detection (for instance light species have higher speed than the heavy one, and this practically eliminates some of them from the useful beam as a proportion of the collision probability).

The present integration is a convenient tool to analyze the response of the mass spectrometer when centering the effusion orifices on the collimation axis at the beginning of the experiments or at any time during an experiment. The profile may be analyzed as a function of the different surface emissions around the effusion orifice as discussed further.

## 2 Results and discussions

### 2.1 Advantages of the restricted collimation device

The first operation that is performed at the beginning of a Knudsen cell mass spectrometric experiment is the centering of the effusion orifice in front of the source aperture when moving the Knudsen cell

furnace. The movement is usually done by manual mechanical jacks but may also be performed by automatic electric jacks and monitoring of the exact positions in a plane perpendicular to the source axis. When the experimenter records the response of the mass spectrometer as a function of the position of the cell, the intensity of monitored ionic species coming from the effusion orifice has generally a round shaped maximum as presented in Figure 14 that can be centered along the axis of the source aperture or not. Chatillon et al [27] attributed a non centered maximum in the total ionic intensity observed as a function of the effusion orifice displacement to the variation of the location of the ionization volume (intercept of the electron and molecular beams) associated probably also to variations in the local electron beam density: indeed, when moving the effusion orifice, the issued molecular beam at the level of the ionization box moved in front of the aperture through which the electrons merged. When the displacement of the molecular beam is towards the electron aperture, we systematically observed an increase of the measured ionic intensity. This feature is directly related to the size of the field aperture which is usually rather large in conventional mass spectrometers (about 5 to 7 mm) compared to the effusion orifice in order to be sure to catch any gaseous species at the initial loading of the Knudsen cell furnace in the mass spectrometer followed by pumping and heating up to the convenient temperature for the first detection of vapors before centering the effusion orifice.

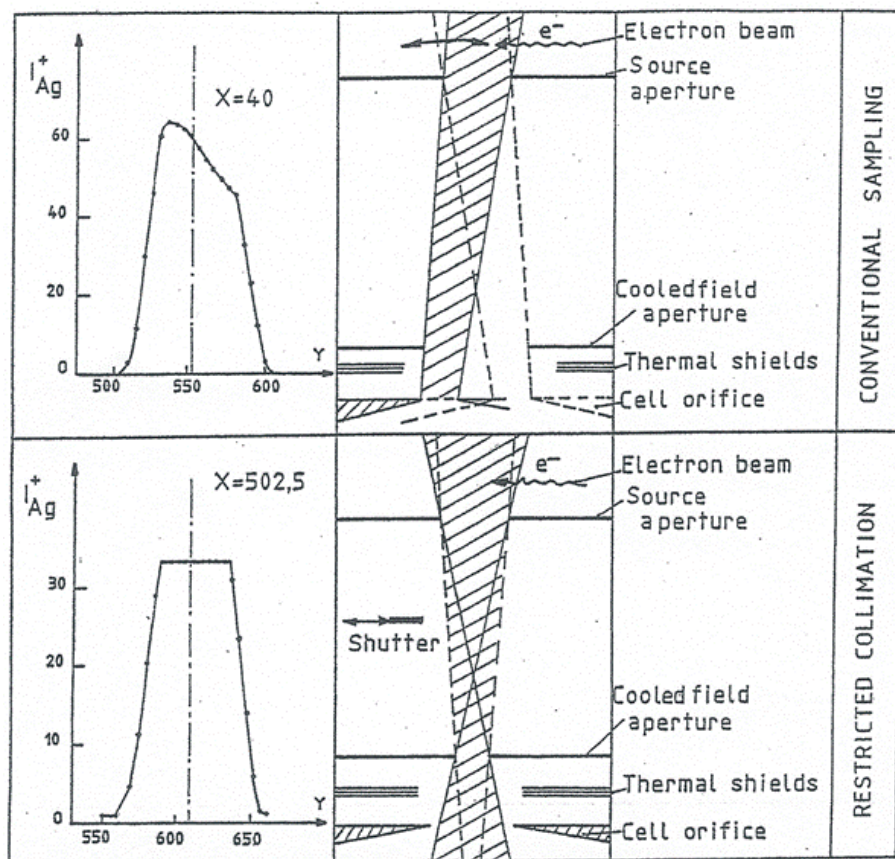


Figure 14 Observation of the ionic intensities when centering the effusion cell along the source aperture axis for conventional or restricted collimation molecular beam sampling.

Tentatively, Chatillon et al [20] used a two filaments source that worked simultaneously to force the response to be round shaped, but this shape was not always obtained and the reproducibility of measurements made with multiple cells not reliable.

Using a restricted collimation device the sampled molecular beam is no longer depending of the position of the effusion orifice but solely on the two apertures – field and source apertures – that are attached to the mass spectrometer structure and consequently fixed. Hence, the response of the mass spectrometer rests constant as long as the penumbra zone is included in the effusion orifice that produces a flat summit, the length of which depends on the admitted clearance (difference  $D_{\text{eff}}-D_p$ ). More the reproducibility of the molecular beam intensity between two different experiments or two different cells in a multiple cell furnace is clearly obtained at the condition that the field aperture may be regularly cleaned since deposit occurs in any experiments from the molecular effused beam.

## 2.2 Restricted collimation in the analysis of surface evaporations

Ionic intensity profiles obtained when centering the effusion orifices may also be performed during the experiment to check either the reliability of the initial centering (especially when using multiple cells) or the modifications in the effusion orifice environment *i.e.* the surface vaporizations. An example of observations performed during multiple cell measurements of activities by Banon et al[28] using a restricted collimation is presented in Figure 15. The multiple cell (four cells) is loaded initially with Ag foils in order to center all the orifices before the measurements on the  $\text{TiO}_x$  samples at higher temperature.

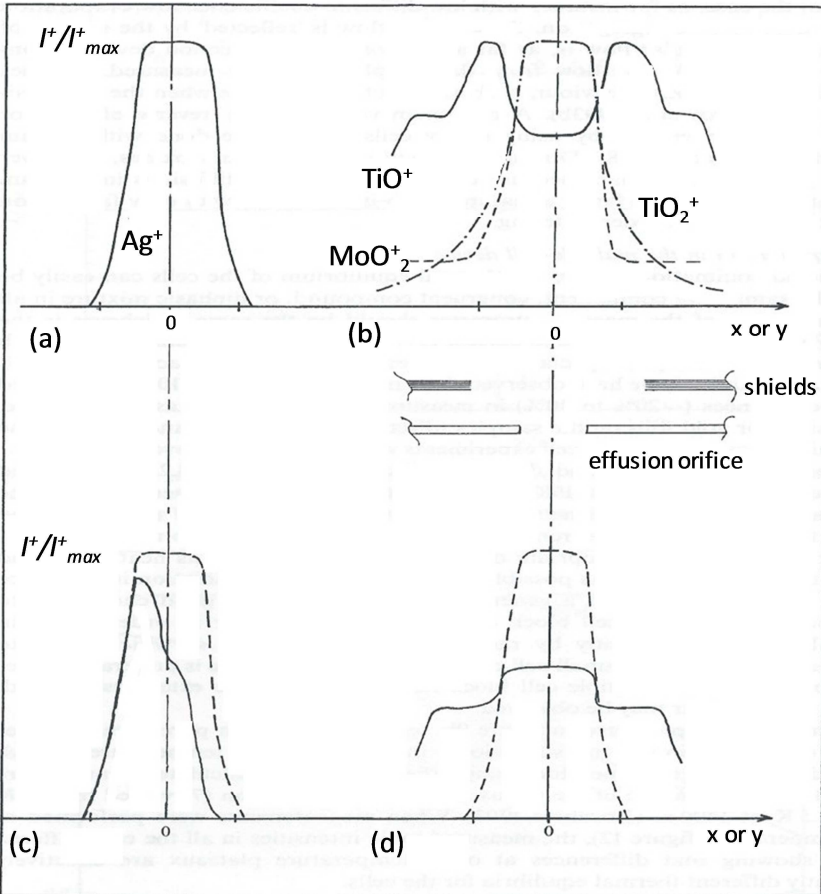


Figure 15 Observations of ionic intensity profiles during the centering of effusion orifices in a multiple cell experiment, samples being titanium oxides. (a): Ag profile from initial silver foil (5 mg) loaded at the surface of each samples and used for the initial centering of each effusion orifices; (b) profile for a cell loaded with a  $TiO_2$  sample. The vapor phase is rich with  $TiO_2(g)$  and an oxide of Mo coming from an interaction of the sample with the Mo crucible, meanwhile the  $TiO^+$  profile reveals  $TiO(g)$  more important outside coming from the other cells with samples rich with  $TiO(s)$ ; (c) this profile shows a partial clogging of the effusion orifice; (d) this profile shows one species clearly coming from the sample and the second species has an important contribution from outside (edges of the orifice).

During the experiment, an anomalous intensity decrease (Figure 15-c) prompted us to center again each orifice to check some modifications in the effusion processes. The observed decrease on one cell is clearly coming from a partial clogging (see Figure 15-c). In Figure 15 (b) and (d) for the  $TiO(g)$  signal as the emission from surface diffusion decreases from the edge, consequently the signal has to decrease. The shoulders here are clearly coming from the other cells richer with  $TiO(g)$  in their gas phase and coming by re-vaporizations in the thermal shields casing. The  $TiO(g)$  pressure is analyzed providing from the samples at the center of the profile (corresponding to the only effusion orifice). The samples in cells are permanently enriched by a back effused flow of the different species coming from the furnace casing. The measured flows (effusion out) can be disturbed by the backflow (reverse effusion) if the vaporization/condensation reactions at the surface of the samples are not at equilibrium that is with a slow kinetics. Malheiros et al[29] observed some anomalous evolution of the activities of  $Na_2O$  as a function of the composition (non-monotonic evolution) in the  $Na_2O-P_2O_5$  binary

system due to reverse effusion of Na(g) provided by the other cells and not totally equilibrated with the sample.

### 2.3 Surface evaporation contribution analysis capabilities

The numerical integration as published by Nuta and Chatillon[23] has been developed in view of calculating the profiles during the centering of the effusion cells. The surface emissivity around the effusion edges – related to the saturated emissivity = 1 at the effusion orifice – can take two different values as presented at the beginning of this work: practically constant value when re-vaporizations come from the thermal shields reflections or a deep profile due to surface diffusion from the orifice edges (see figures 6 and 7 and Chatillon et al[9]). The calculated impact of these two surface evaporations are presented in Figure 16 and Figure 17.

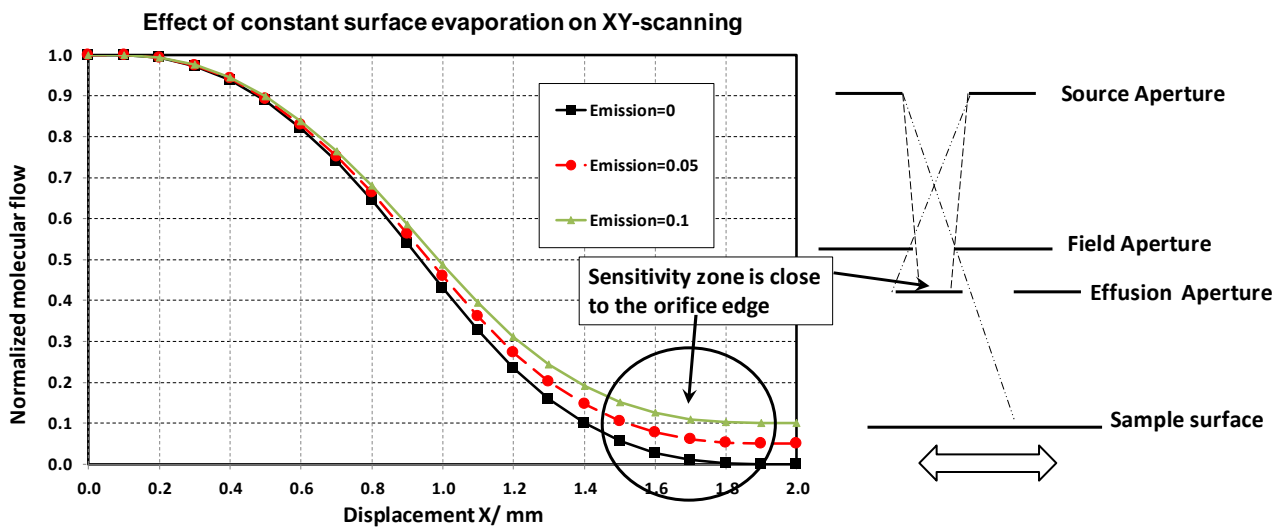


Figure 16 Calculation of the mass spectrometer response when centering the effusion orifice for a “pure” effusion process (Emission=0 for outside surfaces), or for effusion + surface vaporization from the lid around the effusion orifice. The surface emission is referred to 1 for the effusion orifice (saturated vapors).

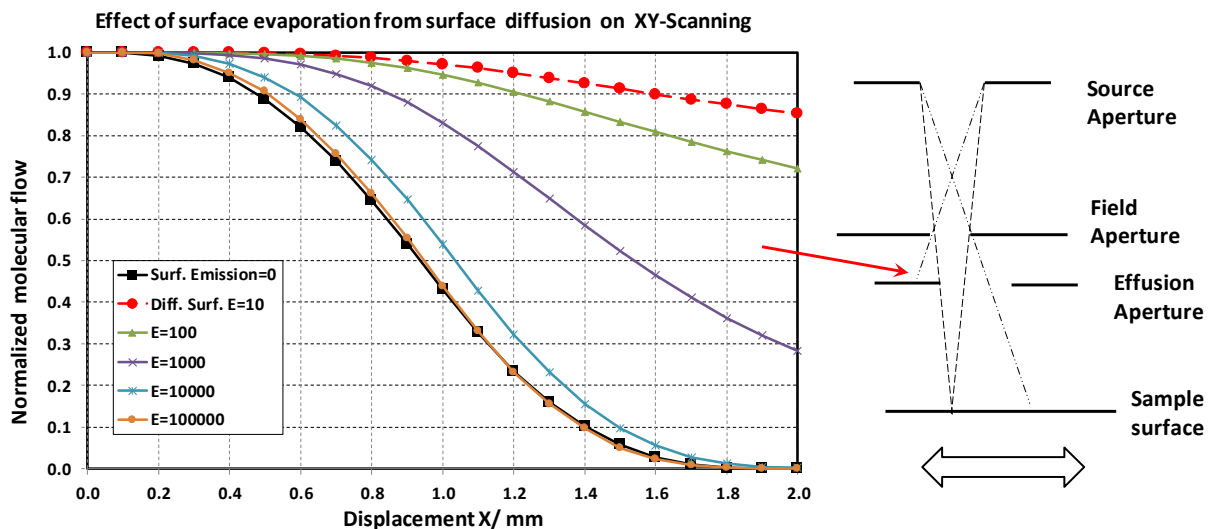


Figure 17 Calculation of the mass spectrometer response when centering the effusion orifice for a “pure” effusion process (Emission = 0 for outside surfaces), or for effusion + surface vaporization from surface diffusion at the effusion orifice edge. The surface emission is referred to 1 for the effusion orifice (saturated vapors).

The zones convenient for detection of these surface contributions are clearly different for these two different surface vaporizations: - (i) constant emissivity will be detected accurately when the penumbra zone leaves the edge of the effusion orifice, - (ii) meanwhile for the surface diffusion contribution the sensitive zone is when the penumbra zone just start to look at the edge of the orifice till the middle of the response peak height.

### 3 Conclusion and perspectives

The present paper has summarized the different causes leading to surface vaporization that cause spurious contributions to the genuine effusion in the Knudsen method for determinations of vapor pressures at high temperature. These contributions have two origins: - (i) first the effused molecules that established a steady-state pressure in the thermal shields casing as used in resistance furnaces. These contributions can be avoided when using HF heating and no thermal shields, devices that have been in use in the Knudsen method either with mass loss or target collection, - (ii) second the molecules that come from the edge of the orifice by surface diffusion and then vaporize. This phenomenon is always occurring due to chemical potential discontinuity at the orifice, and can be minimized when using different materials for the cells lids. The calibration of the effusion flow by mass loss remains sensitive to this surface diffusion flow and Winterbottom et al[12] quoted that the competition between the genuine effusion flow and the surface diffusion flow must disturb significantly the second law results.

The accurate positioning as used for multiple cell activity measurements (cf. Heyrman et al [30]) allows the recording of centering profiles and the further analysis of these profiles in view of the evaluation of the type of surface contributions as well as their evaluation relatively to the genuine effusion. This

systematic analysis may open the way to explain some anomalous data in the determinations of partial pressures by Knudsen Cell Mass Spectrometry and consequently improve the reliability of the method.

#### 4 References

- [1] E.D. Cater, The effusion method at the age 69, in: J.W. Hastie (Ed.) Xth Materials research symposium on "Characterization of High Temperature Vapors and Gases", National Institute of Standards and Technology, Gaithersburg, MD, USA, 1979, pp. 3-38.
- [2] M.G. Ingrham, J. Drowart, Mass Spectrometry Applied to High Temperature Chemistry, High Temperature Technology, McGraw Hill, N.Y., 1959, pp. 219-240.
- [3] J. Drowart, C. Chatillon, J. Hastie, D. Bonnell, High-Temperature Mass Spectrometry: Instrumental Techniques, Ionisation Cross-Sections, Pressure Measurements, and Thermodynamic Data, J. Pure Appl. Chem., 77 (2005) 683-737.
- [4] M. Knudsen, Die Gesetze der Molekularströmung und der inneren Reibungsströmung der Gase durch Röhren, Annalen der Physik, 29 (1909) 75-130.
- [5] J.-L. Vassent, A. Marty, B. Gilles, C. Chatillon, Angular distribution of molecular beams and homogeneous layer growth: optimization of geometrical parameters in molecular beam epitaxy., Vacuum, 64 (2002) 65-85.
- [6] C. Chatillon, C. Sénillou, M. Allibert, A. Pattoret, High temperature studies by mass spectrometry: Device for measurements using multiple effusion cells., Rev. Sci. Instr., 47 (1976) 334-340.
- [7] C. Chatillon, M. Allibert, R. Moracchioli, A. Pattoret, High temperature thermodynamical studies by mass spectrometry. Use of heat pipe devices to maintain isothermal conditions in effusion cells., J. Appl. Phys., 47 (1976) 1690-1693.
- [8] S. Dushman, Scientific Foundations of Vacuum Technique, John Wiley & Sons, N. Y. , 1958.
- [9] C. Chatillon, M. Allibert, A. Pattoret, High Temperature Thermodynamic Studies by Mass Spectrometry: Effect of Surface Evaporation Contributions on the Representativity of Molecular Beam Sampling High Temp. Sci., 8 (1976) 233-255.
- [10] M. Tmar, C. Chatillon, Refinement of the vapor pressures in equilibrium over the InP and InAs compounds by mass spectrometry., J. Chem. Thermodynamics, 19 (1987) 1053-1063.
- [11] W.L. Winterbottom, Vapor-Solid Interactions and the Effusion Oven. I. The Total Effusion Current through a Cylindrical Orifice, J. Chem. Phys., 47 (1967) 3546-3556.
- [12] W.L. Winterbottom, J.P. Hirth, Diffusional Contribution to the Total Flow from a Knudsen Cell, J. Chem. Phys., 37 (1962) 784-793.
- [13] J.W. Ward, R.N.R. Mulford, M. Kahn, Study of Some Parameters Affecting Knudsen Effusion. I. Experimental Tests of the Validity of the Cosine Law as a function of Cell and Sample Geometrics and Materials, J. Chem. Phys., 47 (1967) 1710 -1717.
- [14] J.W. Ward, R.N.R. Mulford, M. Kahn, Study of Some Parameters Affecting Knudsen Effusion. II. A Monte Carlo Computer Analysis of Parameters Deduced from Experiment, J. Chem. Phys., 47 (1967) 1718 - 1723.
- [15] J.W. Ward, Study of Some of the Parameters Affecting Knudsen Effusion. V. Free-Path Considerations in Small Knudsen Cells, J. Chem. Phys., 49 (1968) 5129 - 5132.
- [16] J.W. Ward, M.V. Fraser, Study of the Parameters Affecting Knudsen Effusion. IV. Monte Carlo Analyses of Channel Orifices, J. Chem. Phys., 50 (1969) 1877-1882.
- [17] J.W. Ward, R.L. Bivins, M.V. Fraser, Monte Carlo Simulation of Specular and Surface Diffusional Perturbations to Flow from Knudsen Cell, J. Vac. Sci. Technol, 7 (1970) 206-210.
- [18] J. Drowart, A. Pattoret, S. Smoes, Mass Spectrometric studies of the Vaporization of refractory compounds, Proceedings of the British Ceramic Society, 8 (1967) 67-89.

- [19] A. Pattoret, Etudes thermodynamiques par spectrometrie de masse sur les systemes uranium-oxygene et uranium-carbone, Faculté de sciences, Université Libre de Bruxelles Bruxelles, 1969, pp. 245.
- [20] L. Martin-Garin, C. Chatillon, M. Allibert, Mass spectrometric measurements of activities in liquid Ag-Ge alloys: critical assessment of the thermodynamics of the Ag-Ge system and short distance order, *J. Less-Com. Met.* , 63 (1979) 9-23.
- [21] K. Motzfeldt, The Thermal Decomposition of Sodium Carbonate by the Effusion Method, *J. Phys. Chem.* , 59 (1955) 139-147.
- [22] P. Morland, C. Chatillon, P. Rocabois, High Temperature Mass Spectrometry Using the Knudsen Effusion Cell. .I. Optimization of Sampling Constraints on the Molecular Beam, *High Temp. & Mat. Sci.*, 37 (1997) 167-187.
- [23] I. Nuta, C. Chatillon, Knudsen cell mass spectrometry using restricted molecular beam collimation. I. Optimization of the beam issued from the vaporizing surface, *Rapid Commun. Mass Spectrom.* 29 (2015) 10 - 18.
- [24] I. Nuta, C. Chatillon, Erratum to: "Knudsen cell mass spectrometry using restricted molecular beam collimation. I. Optimization of the beam issued from the vaporizing surface", *Rapid Commun. Mass Spectrom.* 31 (2017) 1-2.
- [25] M.J. Radke, N.S. Jacobson, Monte Carlo Simulation of a Knudsen Effusion Mass Spectrometer Sampling System, NASA-TM-2016 -219118, Glenn Research Center, Cleveland, Ohio 44135 (USA), 2016, pp. 23 pp.
- [26] M.J. Radke, N.S. Jacobson, E.H. Copland, Monte Carlo simulation of a Knudsen effusion mass spectrometer sampling system, *Rapid Commun. Mass Spectrom.* , 31 (2017) submitted.
- [27] C. Chatillon, L.F. Malheiros, P. Rocabois, M. Jeymond, High temperature mass spectrometry using the Knudsen cell. II - Technical constraints in the multiple-cell method for activity determinations., *High Temp. High Press.*, 34 (2002) 213-233.
- [28] S. Banon, C. Chatillon, M. Allibert, High temperature mass spectrometric study of thermodynamic activities in solid TiO-TiO<sub>2</sub> and liquid Ti<sub>2</sub>O<sub>3</sub>-TiO<sub>2</sub> systems., *High Temp. Sci.*, 15 (1982) 105-128.
- [29] L.F. Malheiros, C. Chatillon, M. Allibert, High temperature mass spectrometric study of the Na<sub>2</sub>O-P<sub>2</sub>O<sub>5</sub> and Na<sub>2</sub>O-P<sub>2</sub>O<sub>5</sub>-SiO<sub>2</sub> systems. Activity determination by the multiple Knudsen-cell method., *High Temp. High Press.*, 25 (1993) 35-51.
- [30] M. Heyrman, C. Chatillon, H. Collas, J.-L. Chemin, Improvements and new capabilities for the multiple Knudsen cell device used in high temperature mass spectrometry, *Rap. Comm. Mass Spectrom.*, 18 (2004) 163-174.